International Symposium
On Turbulence and Shear Flow
Phenomena (TSFP-9)
June 30 - July 3, 2015 *Melbourne, Australia*

INERTIAL LOGARITHMIC LAYER PROPERTIES AND SELF-SIMILAR MEAN DYNAMICS

J.C. Klewicki
Department of Mechanical Engineering
University of Melbourne
Melbourne, VIC 3010, Australia
klewicki@unimelb.edu.au

C.T. Morrill-Winter
Department of Mechanical Engineering
University of Melbourne
Melbourne, VIC 3010, Australia
caleb.morrillwinter@gmail.com

A. Zhou
Department of Mechanical Engineering
University of New Hampshire
Durham, NH 03824, USA
ank38@wildcats.unh.edu

ABSTRACT

Turbulent boundary layers contain a region where the mean velocity profile is well-approximated by a logarithmic function. This region is often viewed as constituting an inertial sublayer in physical space. Empirical evidences indicate that a number of other statistical properties exhibit characteristic behaviors on this inertial domain. The present study continues the investigation of these properties and their correlation with the self-similar structure admitted by the mean dynamical equation. Particular emphases pertain to the properties on the inertial layer, the bounds of the domain where these characteristic properties exist, and how these bounds compare with the analytically estimated bounds of the inertial self-similar region.

INTRODUCTION

The statistical structure of turbulent fluctuations in the canonical turbulent wall-flows exhibit distinctive properties in the domain where the mean velocity is well-approximated by a logarithmic function of the wall-normal distance. The present study is broadly concerned with the nature of these properties, and the physical and mathematical attributes that connect them to the existence and bounds of the logarithmic sub-domain. Key physical features are that the domain of interest is internally positioned such that the direct influences of either the inner or outer boundary conditions diminish with increasing Reynolds number, and concomitantly, the associated dynamics on this domain are physically dominated by inertial momentum transport mechanisms. Because they provide mathematically and physically precise specifications for the onset and extent of the inertial domain, recent analyses directed toward revealing properties admitted by the mean momentum equation provide a cogent basis for describing and interpreting statistical structure.

Toward this purpose, this Introduction first provides an overview of recent empirical observations that correlate with the onset and extent of the inertial region. It then provides a description of an analysis framework that is grounded in the properties inherent to the scaling structure associated with the mean momentum equation. This framework provides a basis for interpreting experimental observations within the context of self-similar behaviours attributable to mean dynamical structure.

Previous Empirical Observations

The present effort builds on previously observed statistical features, and their apparent correlation with the self-similar structure of the mean momentum equation. Some of these statistical features are associated with the onset of the logarithmic layer, while others reflect the self-similar nature of the turbulence on the inertial domain. Owing to page limitations, only a subset of the measures mentioned below are considered in the present analyses.

Beyond the position where the mean velocity profile most rapidly approximates logarithmic dependence, indicators of log layer onset include the position of the mid-layer peak in the streamwise velocity (u) spectra, the position of the apparent and emerging mid-layer broadband peak in the streamwise velocity variance, $\langle u^2 \rangle$, the zero-crossing of the low frequency modulation correlation function (physically associated with the so-called 'superstructures, e.g. Mathis et al., 2009), and similarly, the mid-layer zero-crossing of the streamwise velocity fluctuation skewness profile, $S(u)$.

Two of the three measures of emerging self-similar behaviour on the inertial domain studied by Zhou and Klewicki (2015) are considered herein. One is associated with the attached eddy hypothesis-based prediction that with increasing Reynolds number, δ^+, the $\langle u^2 \rangle^+$ profile becomes a logarithmically decreasing function of y^+ over the domain of logarithmic increasing in U^+ (Marusic et al., 2013). (Here a superscript + denotes normalization using ν and u_τ, the kinematic viscosity and friction velocity, respectively, and δ is the boundary layer thickness.) Evidence of this logarithmic dependence in $\langle u^2 \rangle^+$ was subsequently extended and empirically supported by Meneveau and Marusic (2013), and is generalized by

Table 1. Leading order balances and layer width scalings associated with (2). MI, TI and VF respectively denote the mean inertia, turbulent inertia, and mean viscous force terms in (2). Values in parentheses (third column) denote the approximate length units for each layer.

Layer	Magnitude ordering	Δy increment
I	$\|\text{MI}\| \simeq \|\text{VF}\| \gg \|\text{TI}\|$	$O(\nu/u_\tau)$ (≤ 3)
II	$\|\text{VF}\| \simeq \|\text{TI}\| \gg \|\text{MI}\|$	$O(\sqrt{\nu\delta/u_\tau})$ $(\simeq 1.6)$
III	$\|\text{MI}\| \simeq \|\text{VF}\| \simeq \|\text{TI}\|$	$O(\sqrt{\nu\delta/u_\tau})$ $(\simeq 1.0)$
IV	$\|\text{MI}\| \simeq \|\text{TI}\| \gg \|\text{VF}\|$	$O(\delta)$ $(\rightarrow 1)$

$$\langle (u^+)^{2p} \rangle^+ = D_p(\delta^+) - A_p \ln(y^+) \qquad (1)$$

where p indicates the order of the even statistical moment. Zhou and Klewicki showed that, to within data scatter, the domain where (1) holds falls within the bounds where the mean dynamics adhere to a self-similar structure consistent with a logarithmic U^+ profile, see below.

A second measure of inertial layer self-similarity is associated with the so-called diagnostic plot, (Alfredsson and Orlu 2010, Alfredsson et al. 2011). Empirical observations indicate that the plot of $\langle u^2 \rangle^{1/2}/U(y)$ versus $U(y)/U_\infty$ exhibits a linear dependence over a region beyond the peak in the Reynolds stress profile. Thus, it is a statistical measure of the intrinsic self-similarity between the mean velocity and the streamwise velocity fluctuations. Zhou and Klewicki (2015) found that the domain where this linear dependence is observed closely corresponds with where the mean momentum equation admits its self-similar form.

Elements of the Theoretical Framework

The inner-normalized mean streamwise momentum equation for turbulent boundary layer flow in the x direction over a flat plate located at $y = 0$ is given by

$$\left(U^+ \frac{\partial U^+}{\partial x^+} + V^+ \frac{\partial U^+}{\partial y^+} \right) - \frac{\partial T^+}{\partial y^+} = \frac{\partial^2 U^+}{\partial y^{+2}} \qquad (2)$$

where $T^+ = -\langle uv \rangle^+$. From left to right, the terms in (2) represent the the mean flow inertia (MI), the mean effect of turbulent inertia (TI), and the mean viscous force (VF). Each term in (2) is of leading order of some portion of the boundary layer, but not necessarily everywhere. The leading order balances across $0 \leq y \leq \delta$ have been analytically determined (to order of magnitude), and empirically verified. These balances are summarized in table 1, (Wei et al., 2005, Fife et al., 2009).

From table 1 note that the VF term loses leading order at $y \simeq 2.6\sqrt{\nu\delta/u_\tau}$, or equivalently at $y^+ \simeq 2.6\sqrt{\delta^+}$. This position marks the onset of the inertial domain. It has been shown that the structure reflected in table 1 arises from (2) admitting an invariant form across a hierarchy of scaling layers that spans from $y^+ \simeq 7$ to $y/\delta \simeq 0.5$, e.g., Klewicki (2013). Thus, the inertial portion of this underlying hierarchy resides within the bounds $2.6\sqrt{\delta^+} \leq y^+ \leq 0.5\delta^+$.

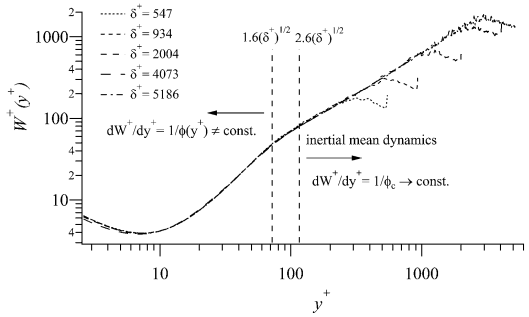

Figure 1. Distribution of $W^+(y^+)$ for channel flows. Profiles at $\delta^+ = 547, 934$ and 2004 are from the study of Hoyas and Jiménez (2006). The profile at $\delta^+ = 4073$ is from Pirozolli (2014), and the profile at $\delta^+ = 5186$ is from Lee and Moser (2015). Vertical lines denoting the beginning and end of layer III are shown for $\delta^+ = 2004$.

The distribution of its layer widths, $W^+(y^+)$, is a defining characteristic of the layer hierarchy. Namely, when u_τ and $W(y)$ are used to normalize (2) this equation becomes invariant and parameter free. Given data uncertainties, $W^+(y^+)$ is most readily computed using $W^+ = (-\partial^2 U^+/\partial y^{+2})^{-1/2}$, although other alternatives exist (Fife et al., 2009, Klewicki, 2013). Figure 1 shows W^+ distributions for channel flows up to $\delta^+ \simeq 5200$. Note that on the domain between $y^+ \simeq 2.6\sqrt{\delta^+}$ and the estimated upper bound of the layer hierarchy, $y/\delta \leq 0.5$, $dW/dy \rightarrow$ const $= \phi_c^{-1}$, while closer to the wall $dW/dy \neq$ const. Because (2) admits (to leading order) an invariant form on the layer hierarchy, its solutions on this domain become increasingly self-similar as $\delta^+ \rightarrow \infty$. The function ϕ (Fife similarity parameter, Klewicki, 2013) is a coordinate stretching that renders solutions to (2) invariant for changes in δ^+.

Two types of self-similarity are operative on the layer hierarchy, with the simpler associated with ϕ approaching a constant, ϕ_c (see figure 1). This exposes an equation-based origin for the *distance from the wall* scaling that is, for example, central to Townsend's notion of an attached eddy, and associated with the emergence of a logarithmic mean profile as $\delta^+ \rightarrow \infty$, Fife et al. (2009). Its location is also in accord with the recent findings of Marusic et al. (2013) that the onset of the inertial logarithmic layer moves to increasing y^+ values in proportion to $\sqrt{\delta^+}$.

RESULTS

The primary laboratory data sets used are from experiments in the Flow Physics Facility (FPF) wind tunnel at the University of New Hampshire, and the High Reynolds Number Boundary Layer Wind Tunnel (HRNBLWT) at the University of Melbourne. These are complemented with data from field experiments at the Surface Layer Turbulence and Environmental Science Test (SLTEST) facility in Utah's west desert, and other data from the literature. Distinctive attributes of the measurements used are that they extend up to high Reynolds numbers and maintain good spatial resolution. The laboratory measurements were acquired using hot-wire sensors (0.5mm long, 2.5μm diameter) that had a length that ranged between 5 and 16 viscous units, while the 1.0mm, 5.0μm dia. sensors used at the SLTEST site had an inner normalized length that was always less than 10. The present analyses focus on measures that char-

acterize the onset and extent of, and the properties within, the logarithmic inertial domain. These are compared with previous measurements, and with the properties of the self-similar inertial domain determined via analysis of (2).

Inertial Layer Properties

The iconic feature of the spatial inertial sublayer of wall-turbulence is an inner-normalized mean velocity profile that is well-approximated by

$$U^+ = \frac{1}{\kappa}\ln(y^+) + B \tag{3}$$

where κ (taken to equal 0.39) is the von Kármán constant, and B is a constant that depends on the nature of the surface – taken to equal 4.3 for the smooth-wall flows considered. Figure 2 plots the mean profiles of the eight FPF and HRNBLWT flows listed in table 2. Following Marusic et al. (2013), the logarithmic part of (3) is subtracted from the data such that the inertial region of interest is represented by a constant value equalt to B. Using this representation, Marusic et al. found the logarithmic region to be bounded by $C_1\sqrt{\delta_{99}^+} \le y^+ \le C_2\delta_{99}^+$, where $C_1 \simeq 3.4$ and $C_2 \simeq 0.19$. Overall, the present results are consistent with these findings, in that they suggest that the lower boundary of the inertial region scales on a length that is intermediate to ν/u_τ and δ, while the upper boundary more clearly scales on δ. Like the results reported by Vincenti et al. (2013), the data of figure 2 are not of sufficient fidelity to unambiguously locate the inertial layer onset. Here we also note that the previous data seem to indicate that the data approach the constant plateau from above a low δ^+ and from below at high δ^+, and thus this feature also complicates the precise identification of the beginning of the logarithmic layer using this method.

Because it relates to the turbulent fluctuations, (1) is likely to be a more sensitive measure of the spatial position of the inertial domain. With this in mind, the present new measurements from the FPF and HRNBLWT were analyzed in same way that Zhou and Klewicki (2015) treated the earlier 1.0mm sensor FPF measurements of Vincenti et

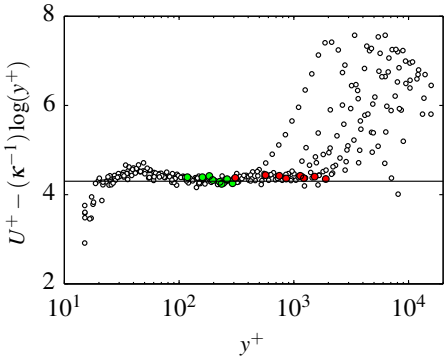

Figure 2. Deviation of the measured mean velocity profile from the logarithmic line. Here a value of $\kappa = 0.39$ was used. The horizontal line denotes a value of 4.3. Per the analyses of Marusic et al. (2103), the green and red circles show the locations corresponding to $y^+ = 2.6\sqrt{\delta^+}$ and $y^+ = 0.15\delta^+$, respectively.

Table 2. Slope coefficients, A_p, of the even moment curve fits for $2058 \le \delta^+ \le 12701$. Bold face δ^+ are from the FPF, others are from the HRNBLWT.

δ^+	A_1	A_2	A_3	A_4	A_5
2058	-1.03	-1.61	-2.07	-2.42	-2.70
3771	-1.28	-1.94	-2.41	-2.70	-2.88
4997	-1.32	-2.05	-2.63	-3.09	-3.45
5704	-1.18	-1.83	-2.36	-2.80	-3.16
7584	-1.37	-2.18	-2.87	-3.47	-4.00
8162	-1.25	-1.93	-2.49	-2.92	-3.24
10102	-1.29	-2.02	-2.60	-3.04	-3.35
12701	-1.34	-2.13	-2.78	-3.29	-3.68
Average	-1.26	-1.96	-2.53	-2.97	-3.31

al. (2013). This analysis generally adhered to the procedure described by Meneveau and Marusic (2013). Here the profiles of the even moments of the u fluctuations (up to tenth moment) were computed, and a logarithmic line was fit to the data in the outer region of decreasing moment magnitude. Different from Meneveau and Marusic, however, the present data were fit over the domain $2.6\sqrt{\delta^+} \le y^+ \le 0.3\delta^+$, as in the analysis of Zhou and Klewicki.

The results of figure 3 demonstrate this process at $\delta^+ \simeq 8000$ measurements from the FPF and HRNBLWT, while the entries in table 2 summarize the overall results of the analysis. The results for the A_p in the table are in good agreement with of Meneveau and Marusic and Zhou and Klewicki. For example, the present data yield an average value for $A_1 = 1.26$. This is very close to the value of 1.27 reported by Zhou and Klewicki, and is identical to the value found by Meneveau and Marusic. It is interesting to note, however, that the results from table 2 seem to suggest that at comparable Reynolds numbers, the slope magnitudes from the FPF are slightly larger than those derirved from the HRNBLWT. As exemplified by the results in figure 3, the data from the FPF exhibit slightly greater scatter than those from the HRNBLWT. This is primarily attributable to larger non-dimensional averaging time afforded by the HRNBLWT experiments. Figure 3 also exemplifies and reinforces the general finding of Zhou and Klewicki that the region of most convincing logarithmic decrease lies within the theoretical bounds of $2.6\sqrt{\delta^+} \le y^+ \le 0.5\delta^+$. Overall, examination of the individual curves underlying the results of table 2 indicates that with increasing δ^+ the data begin their logarithmic decrease at a position that increasingly approaches the position where the VF term in (2) loses leading order, i.e., at the outer edge of layer III, see table 1. Similarly, at any fixed δ^+, this same lower limit seems to be approached with increasing moment.

The mean momentum equation based analysis mentioned in the Introduction support the assertion that the properties of the inertial logarithmic region derive from an underlying self-similar structure. Empirical observations of the outer region behavior of the diagnostic plot of Alfredsson and Orlu (2010) are consistent with this. Specifically, the (approximately) invariant linear region of diagnostic plot reflects a self-similar relationship between the mean velocity and the fluctuations about this mean.

Figure 4 presents the modified diagnostic plot of the FPF and HRNBLWT data of table 2. As is apparent, the

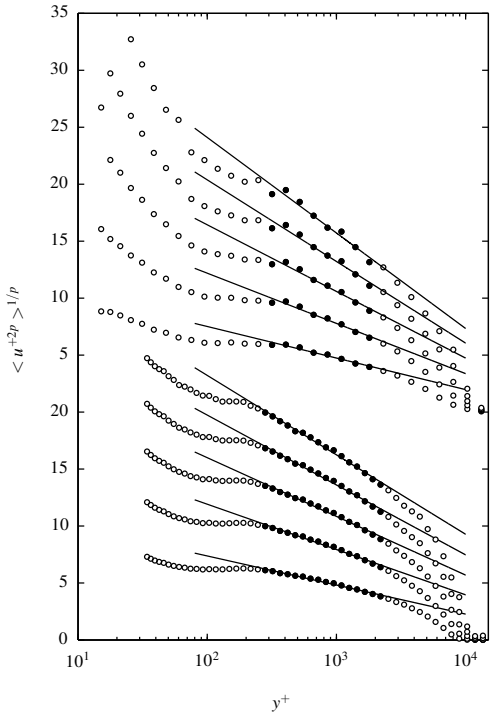

Figure 3. Even statistical moment profiles (2p = 2, 4, 6, 8, 10) of u time-series at $\delta^+ = 7584$ (top) and $\delta^+ = 8162$ (bottom). Profile at $\delta^+ = 7584$ is from the FPF and the profile at $\delta^+ = 8162$ is from the HRNBLWT. Solid lines represent average values in table 2. Filled symbols reside between $y^+ \simeq 2.6\sqrt{\delta^+}$ and $y/\delta \simeq 0.3$.

data from the two facilities exhibit a compelling level of agreement, and interestingly, close examination reveals all of the profiles exhibit a noticeable deviation from purely linear behaviour; suggesting that the linear behaviour is an approximation, while the self-similarity is robust. The linear region fit derived from the present data, $u'/U = -0.269(U/U_\infty) + 0.296$, is in very good, but not identical, agreement with the earlier fits given by Alfredsson et al. (2011) and Zhou and Klewicki (2013). Somewhat distinct from the results of Zhou and Klewicki, the present results also suggest that the linear approximation begins a little before $y^+ = 2.6\sqrt{\delta^+}$, and ends a little beyond $y^+ = 0.5\delta^+$. These bounds are indicated by the red-filled data points in figure 4. A potential explanation for this observation is that both u' and U deviate from the their characteristic behavior on the inertial domain such that their ratio continues to adhere (approximately) to a straight line even beyond the bounds of self-similar domain indicated by the theory. More generally, upon examining the diagnostic plot for a significant number of profiles, it seems apparent that while its invariance is clearly robust, it is not a particularly sensitive measure of wall-turbulence structure.

Inertial Layer Onset

The results presented thus far provide relatively clear evidence that the upper bound of the inertial logarithmic region scales with δ^+. The evidence that the lower boundary scales with $\sqrt{\delta^+}$ is, however, more ambiguous. As mentioned in the Introduction, previous observations suggest

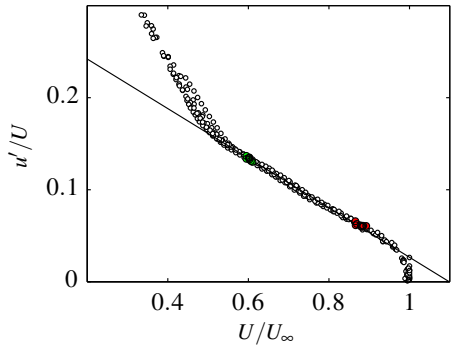

Figure 4. Modified diagnostic plot of the experiments represented in table 2. The black line represents the average linear fit of the data from all of the profiles between $0.65 \leq U/U_\infty \leq 0.85$; $u'/U = -0.269(U/U_\infty) + 0.296$; prime denotes the rms. The green and red circles show the locations corresponding to $y^+ = 2.6\sqrt{\delta^+}$ and $y^+ = 0.5\delta^+$, respectively.

that a number of statistics are either associated through the theory with the inertial layer, or have been shown to correlate with this onset. Such statistics are now examined.

The evidence for the emergence (with increasing δ^+) of a mid-layer ("outer") peak in the pre-multiplied spectrograms of u is well-established, e.g., Hutchins and Marusic (2007). Furthermore, while existing evidence indicates that the y^+ position of this peak nominally scales with $\sqrt{\delta^+}$, the spatial breadth of this spectral region makes its precise estimation difficult, e.g., Vincenti et al. (2013). Similarly, the evidence pertaining to whether this spectral peak underlies the emergence of a mid-layer peak in the broadband statistic, $\langle u^2 \rangle^+$, remains ambiguous. In either case, however, it is readily surmised that the position of any broadband plateau or peak, must reside just interior to the region of logarithmic decrease depicted in figure 3.

The measurements by Vincenti et al. (2013) between $6000 \leq \delta^+ \leq 20000$ provide evidence in support of a developing $\langle u^2 \rangle^+$ peak. Similarly, while exhibiting more scatter, SLTEST facility based field measurements from the study of Priyadarshana and Klewicki (2004) also suggest the emergence of a peak in $\langle u^2 \rangle^+$. To investigate the δ^+ scaling associated with the location of this peak, figure 5 plots $\langle u^2 \rangle^+$ versus $y^+/\sqrt{\delta^+}$ from the present FPF and HRNBLWT experiments, along with representative profiles $\delta^+ > 6000$ from Vincenti et al. (2013), as well as measurements from the SLTEST site. A number of features are apparent on the plot. It is firstly clear that the laboratory data at most provide relatively subtle evidence of a peak near $y^+/\sqrt{\delta^+} = 2.6$ (also see figure 3), while, even given their scatter, the SLTEST data are much more suggestive of a peak. Secondly, regardless of the existence of an identifiable peak, the data in the peak (plateau) region convincingly align under the $y^+/\sqrt{\delta^+}$ scaling. Lastly, in accord with the profiles of figure 2, these data indicate that the logarithmic decrease reflected in (1) begins slightly beyond $y^+ \simeq 2.6\sqrt{\delta^+}$. Quantifications of the spectral and broadband peak are included in the compilation of figure 6. These include the estimated locations from the FPF (Vincenti et al., 2013), and from the SLTEST facility (Priyadarshana and Klewicki, 2004; Metzger et al., 2007).

Figure 6 provides a summary of quantities that correlate with the transition from a mean dynamical balance in

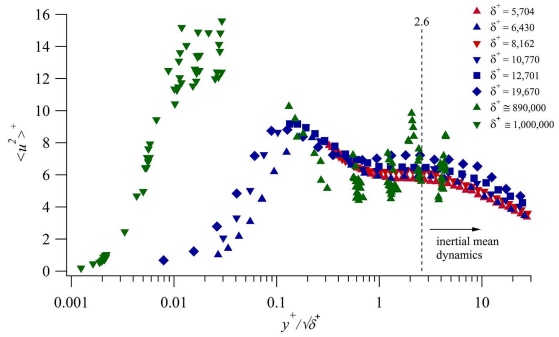

Figure 5. Streamwise velocity variance profiles plotted versus $y^+/\sqrt{\delta^+}$. Red symbols are from the the present HRNBLWT study. Blue symbols are from the present FPF study and Vincenti et al. (2013). The green symbols are from the SLTEST facility; near-wall, Metzger and Klewicki (2001), mid-layer, Priyadarshana and Klewicki (2004).

which the VF term in (2) is leading order to one in which the leading order terms are wholly inertial. As reflected in table 1, the wall-normal location, y_m^+, of the peak in $-\langle uv \rangle^+$ must occur within the bounds of layer III. Because of this, y_m^+ provides a convenient surrogate for the point at which the transition to inertial dynamics occurs (Mehdi et al. 2013). As described by Chin et al. (2014), and shown in figure 6, the DNS of Chin (2011) and the Princeton Superpipe measurements of Hultmark et al. (2013) closely adhere to the theoretically predicted behavior, with the curve fit of data up to $\delta^+ \simeq 1 \times 10^5$ given by $y_m^+ = 1.77\sqrt{\delta^+}$.

Based upon the physical recognition that the TI term changes from a momentum source to momentum sink across layer III, Klewicki et al. (2007) surmised that, independent of Reynolds number, the domain of the inner/outer interaction in the boundary layer on average contains layer III. Relevant to this, Mathis et al. (2009) quantified the correlation coefficient, $R(y^+)$, profile associated with the modulation of the near-wall flow by the inertial layer motions, and subsequent studies have shown that the skewness of the u fluctuations, $S(u)$, is closely related to R (e.g., Mathis et al., 2012; Subrahmanyam and McKeon 2015). In particular, the zero-crossing of either R or $S(u)$ is seen to coincide (on average) with the inertially dominated motions nearest the wall, and thus is physically associated with the transition to inertially dominated mean dynamics. Results in figure 6 include zero-crossing data for both R and $S(u)$. These data come from the FPF measurements of Vincenti et al. (2013), the study of Mathis et al. (2009), FPF and HRNBLWT experiments of table 2, as well as SLTEST facility measurements (Klewicki et al., 2005; Priyadarshana and Klewicki, 2004). Relative to the R data, the δ^+ value has been adjusted to reflect δ_{99}, and thus be consistent with the rest of the data on the plot. Overall, these data indicate that the zero-crossing occurs near to, or possibly just slightly beyond, $y^+ = 2.6\sqrt{\delta^+}$.

The recent extension of the present theory to rough-wall flows by Mehdi et al. (2013) provides a means to further examine the $S(u)$ zero-crossing as a measure of the start of the inertial domain. Here we first note that, in contrast to prevalent thinking, data covering significant ranges in δ^+ and k_s^+ reveal that the mean viscous force generically retains importance above (and often well-above) the roughness crests. Concomitantly, the leading order layer II, III and IV force balance structure described in table 1 is preserved in rough-wall flows. As with the overall dynamical structure, the transition to inertial mean dynamics now depends non-trivially on the combined influences of roughness and Reynolds number. The property that y_m always resides within layer III is, however, preserved. This allows y_m to be used as a surrogate for the transition to inertial mean dynamics. Accordingly, Mehdi et al. (2013) quantified (via empirical curve-fits) the dependence of y_m on the relative scale separations between the inner, roughness, and outer length scales, and used these as a way to demonstrate connections between a number of rough-wall flow features to those in smooth-wall flow. Following this approach, figure 7 presents recently acquired smooth- and rough-wall $S(u)$ zero-crossing measurements from a suite of HRNBLWT experiments covering $3000 < \delta^+ < 30000$ and equivalent sand grain roughnesses covering $23 < k_s^+ < 150$. The results of figure 6 show that the $S(u)$ zero-crossing consistently occurs somewhat beyond y_m, and consistent with this, the results of figure 7 indicate that the measured zero-crossing position nominally correlates with the position equal to $2.3y_m^+$.

CONCLUSIONS

The present study investigated statistical properties of the flow within the inertial sublayer of the turbulent boundary layer, as well as measures of the (approximate) beginning and end points of this inertial domain. These results were compared to, and described within the context of, a description of this inertial domain as developed from consideration of the invariance properties associated with the mean momentum equation. The upper and lower bounds for the inertial domain developed through the theory are $y+ \geq 2.6\sqrt{\delta^+}$ and $y/\delta \leq 0.5$. Comparisons of the empirical measures investigated with this domain specification generally indicate good correlation. It would seem, however, that the quality of the agreement depends upon the sensitivity of the particular statistic to the underlying self-similar structure. That is, some measures, such as the logarithmic decrease in the even moments of u exhibit their characteristic property wholly within the analytical bounds, while others, such as the linear region in the diagnostic plot, provide evidence of extending slightly before and beyond the analytically estimated bounds. Of course, finite Reynolds number and data uncertainties also factor into these considerations.

A number of measures were used to separately estimate the onset of the inertial domain. These exhibit very good agreement with the position $y^+ \simeq 2.6\sqrt{\delta^+}$.

REFERENCES

Alfredsson, H. & Orlu, R. 2010 The diagnostic plot – a litmus test for wall-bounded turbulence data. *European Journal of Mechanics B/Fluids* **29**, 403–406.

Alfredsson, H., Segalini, A. & Orlu, R. 2011 A new scaling for the streamwise turbulence intensity in wall-bounded turbulent flows and what it tells us about the "outer" peak. *Physics of Fluids* **23**, 041702.

Chin, C., Philip, J., Klewicki, J., Ooi, A. & Marusic, I. 2014 Reynolds-number-dependent turbulent inertia and onset of log region in pipe flows. *Journal of Fluid Mechanics* **757**, 747–769.

Fife, P., Klewicki, J. & Wei, T. 2009 Time averaging in turbulence settings may reveal an infinite hierarchy of

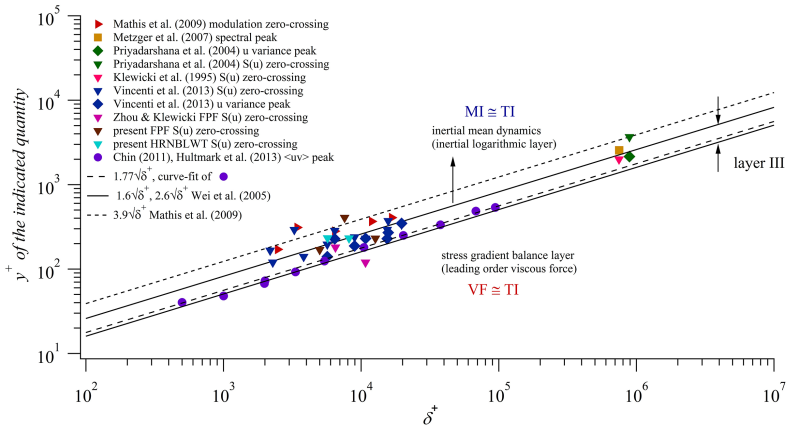

Figure 6. Compilation of empirical measures that correlate with the onset of inertial mean dynamics in smooth-wall flow.

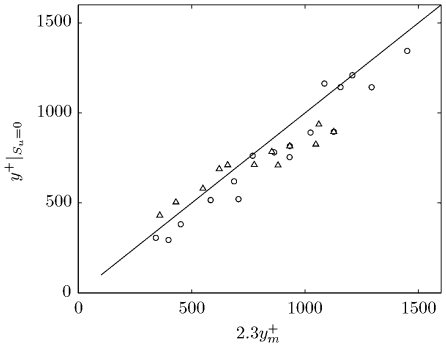

Figure 7. Position of the $S(u)$ zero-crossing versus $2.3y_m^+$ for both smooth-wall (triangles) and sandpaper roughness (circles) experiments conducted in the HRNBLWT. The data cover $3147 \leq \delta^+ \leq 29902$ and rough-walls span $13 \leq k_s^+ \leq 153$. The peak in the Reynolds stress, y_m^+, was estimated using the formula of Mehdi et al. (2013) for $y_m > k_s$.

length scales. *Discrete and Continuous Dynamical Systems A* **24**, 781–807.

Hoyas, S. & Jimenez, J. 2006 Scaling the velocity fluctuations in turbulent channels up to $Re_\tau = 2003$. *Physics of Fluids* **18**, 011702.

Hultmark, H., Vallikivi, M., Bailey, S.C.C. & Smits, A.J. 2013 Logarithmic scaling of turbulence in smooth- and rough-wall pipe flow. *Journal of Fluid Mechanics* **728**, 376–395.

Hutchins, N. & Marusic, I. 2007 Large-scale influences in near-wall turbulence. *Philosophical Transactions of the Royal Society of London, Series A* **365**, 647–664.

Klewicki, J. 2013 Self-similar mean dynamics in turbulent wall flows. *Journal of Fluid Mechanics* **718**, 596–621.

Klewicki, J., Fife, P. & Wei, T. 2009 On the logarithmic mean profile. *Journal of Fluid Mechanics* **638**, 73–93.

Klewicki, J., Fife, P., Wei, T. & McMurtry, P. 2007 A physical model of the turbulent boundary layer consonant with mean momentum balance structure. *Philosophical Transactions of the Royal Society of London, Series A* **365**, 823–839.

Klewicki, J., Metzger, M.M. & Kelner, E. 1995 Statistical structure of the axial velocity fluctuations in a near-neutral atmospheric boundary layer in the immediate vicinity of a mud flats ground plane. Technical Report PFD Rep. 95-01. Univ. Utah, Salt Lake City, UT.

Lee, M. & Moser, R. 2015 Direct numerical simulation of turbulent channel flow up to $Re_\tau \sim 5200$. *Journal of Fluid Mechanics* **in press**.

Marusic, I., Monty, J., Hultmark, M. & Smits, A. 2013 On the logarithmic region in wall-turbulence. *Journal of Fluid Mechanics* **716**, R3–11.

Mathis, R., Hutchins, N. & Marusic, I. 2009 Large-scale amplitude modulation of the small-scale structures in turbulent boundary layers. *Journal of Fluid Mechanics* **628**, 311–337.

Mathis, R., Marusic, I., Hutchins, N. & Sreenivasan, K.R. 2011 The relationship between the velocity skewness and the amplitude modulation of the small scale by the large scale in turbulent boundary layers. *Physics of Fluids* **23**, 121702.

Mehdi, F., Klewicki, J. & White, C. 2013 Mean force structure and its scaling in rough-wall turbulent boundary layers. *Journal of Fluid Mechanics* **731**, 682–712.

Meneveau, C. & Marusic, I. 2013 Generalized logarithmic law for high-order moments in turbulent boundary layers. *Journal of Fluid Mechanics* **719**, R1–11.

Metzger, M., McKeon, B. & Holmes, H. 2007 The near-neutral atmospheric surface layer: turbulence and non-stationarity. *Philosophical Transactions of the Royal Society of London, Series A* **365**, 859–876.

Pirozzoli, S. 2014 Revisiting the mixing-length hypothesis in the outer part of turbulent wall layers: mean flow and wall friction. *Journal of Fluid Mechanics* **745**, 378–397.

Priyadarshana, P. & Klewicki, J. 2004 Study of the motions contributing to the Reynolds stress in high and low Reynolds number turbulent boundary layers. *Physics of Fluids* **16**, 4586–4600.

Subrahmanyam, D. & McKeon, B.J. 2015 Triadic scale interactions in a turbulent boundary layer. *Journal of Fluid Mechanics* **767**, R4–1.

Vincenti, P., Klewicki, J., Morrill-Winter, C., White, C. & Wosnik, C. 2013 Streamwise velocity statistics in turbulent boundary layers that spatially develop to high Reynolds number. *Experiments in Fluids* **54**, 1629–1638.

Wei, T., Fife, P., Klewicki, J. & McMurtry, P. 2005 Properties of the mean momentum balance in turbulent boundary layer, pipe and channel flows. *Journal of Fluid Mechanics* **522**, 303–327.

Zhou, A. & Klewicki, J. 2015 Properties of the streamwise velocity fluctuations in the inertial layer of turbulent boundary layers and their connection to self-similar mean dynamics. *International Journal of Heat and Fluid Flow* **51**, 372–382.